White-light imaging with fractal zone plates

Walter D. Furlan,[1,*] Genaro Saavedra,[1] and Juan A. Monsoriu[2]

[1]*Departamento de Óptica, Universitat de València, E-46100 Burjassot, Spain*
[2]*Departamento de Física Aplicada, Universidad Politécnica de Valencia, E-46022 Valencia, Spain*
[*]*Corresponding author: walter.furlan@uv.es*

Received March 15, 2007; accepted May 9, 2007;
posted June 7, 2007 (Doc. ID 81071); published July 19, 2007

We report the achievement of the first images to our knowledge obtained with a fractal zone plates (FraZPs). FraZPs are diffractive lenses characterized by the fractal structure of their foci. This property predicts an improved performance of FraZPs as image forming devices with an extended depth of field and predicts a reduced chromatic aberration under white-light illumination. These theoretical predictions are confirmed experimentally in this work. We show that the polychromatic modulation transfer function of a FraZP affected by defocus is about two times better than one corresponding to a Fresnel zone plate. © 2007 Optical Society of America

OCIS codes: 050.1970, 340.7440, 110.4850.

Fresnel zone plates are diffractive elements that are essential for forming images in many scientific and technological areas, especially where refractive optics is not available [1–4]. One of the main shortcomings of Fresnel zone plates is their high chromatic aberration. Recently presented, fractal zone plates (FraZPs) [5] have drawn the attention of several research groups working on diffractive optics [6,7] because it has been assumed that they can improve the performance of classical Fresnel zone plates in certain applications where multiple foci are needed. FraZPs also inspired the invention of other photonic structures [7,8]. In spite of their potential applications as imaging elements, until the present only the focusing properties of FraZPs have been considered in the literature. Here we examine the incoherent imaging characteristics of these elements using polychromatic light in the visible range. The performance of FraZPs is compared with conventional Fresnel zone plates of the same focal distances. We found that the FraZP provides an extended depth of field and a reduction of chromatic aberration.

FraZPs can be built by using the same methods and technologies used for conventional Fresnel zone plates. Thus, we begin by tracing a parallelism in the design process between these two elements. As is well known, a Fresnel zone plate consists of alternately transparent and opaque zones whose radii are proportional to the square root of the natural numbers. Thus, it can be generated starting from a 1D compact-supported periodic function $q(\zeta)$ [see for example the binary function in Fig. 1(a)], followed by a change of coordinates $\zeta=(r/a)^2$, and then by a rotation of the transformed function around one of its extremes. The resulting radially symmetric 2D structure is a Fresnel zone plate having a radial coordinate r and an outermost ring of external radius a [see Fig. 1(b)].

In a similar way a FraZP can be constructed by replacing the periodic function $q(\zeta)$ by a function $f(\zeta)$ with fractal profile. In Fig. 1(c) we have represented the 1D binary function associated with a member of the triadic Cantor set developed up to the third stage, $S=3$ [5]. The corresponding FraZP is shown in Fig. 1(d). It is worth mentioning that in the most general case any 1D fractal can be employed to construct a FraZP. A comparison between Figs. 1(a) and 1(c) shows that the minimum distance between the zones of the fractal binary function $f(\zeta)$ coincides with a half-period of the periodic function $q(\zeta)$. This distance defines the width of the outermost zones in the zone plates, Δr, and thus limits their ultimate spatial resolution. However, as the focal length of a Fresnel zone plate is inversely proportional to the wavelength, for wideband illumination its longitudinal chromatic aberration [see Fig. 2(a)] severely limits its imaging performance. We will see that FraZPs can partially overcome this limitation.

We calculate the monochromatic irradiances along the optical axis provided by the zone plates, using the Fresnel diffraction formula:

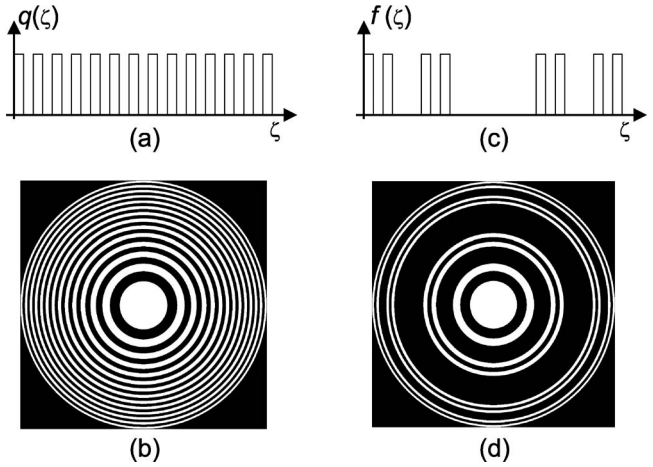

Fig. 1. FraZP design. The same procedure can be followed in designing fractal and Fresnel zone plates. It consists of three steps. (a) A Fresnel zone plate starts from a binary 1D compact supported function $q(\zeta)$. After the change of variables $\zeta=(r/a)^2$, the resulting function, which is periodic in the new coordinate, is rotated around the origin. The result is the zone plate represented in (b). (c) The originating function for the FraZP is a fractal binary 1D function $f(\zeta)$. In this case it is a triadic Cantor set for stage 3 (see Ref. [5] for details). (d) The change of variables and rotation performed to obtain (b) now results in a FraZP.

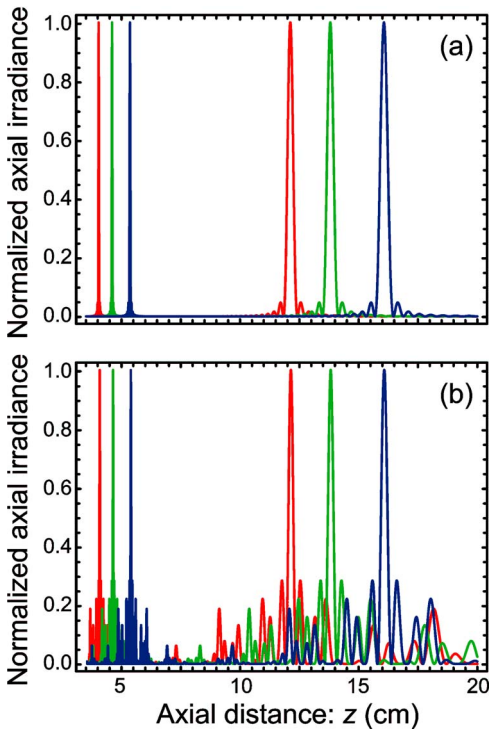

Fig. 2. (Color online) Point spread functions for different wavelengths. The axial irradiances were computed by using Eq. (1) for $a=2.52$ mm and $\lambda=647$ nm (red or medium gray), $\lambda=568$ nm (green or light gray), and $\lambda=488$ nm (blue or dark gray). (a) Fresnel zone plate of 81 zones. (b) FraZP of the same focal distance. The FraZP in this case was obtained for a triadic Cantor set like the one in Fig. 1(d) but developed up to stage 4.

$$I(z)=\left(\frac{2\pi}{\lambda z}\right)^2\left|\int_0^a p(r)\exp\left(-i\frac{\pi}{\lambda z}r^2\right)r\mathrm{d}r\right|^2, \qquad (1)$$

where $p(r)$ is the 2D circularly symmetric pupil function that describes the zone plate in canonical polar coordinates. In Fig. 2 we represented the axial irradiances provided by a Fresnel zone plate and a FraZP of the same focal length computed for three different wavelengths in the visible spectrum. As can be seen, the principal lobes of the different foci provided by a FraZP coincide in the axial position with those obtained with a conventional Fresnel zone plate, but the FraZP produces a sequence of subsidiary foci around each major focus following the fractal structure of the FraZP itself. In general, the position, the intensity and the 3D shape of the focal spot depend on the fractal level and on the lacunarity [9] of the encoded fractal function $f(\zeta)$. In all cases these subsidiary foci of the FraZP provide an extended depth of focus for each wavelength that partially overlaps with the other ones, creating an overall extended depth of focus that is less sensitive to chromatic aberration.

We have experimentally tested the imaging capabilities of FraZPs under white-light illumination and compared their performance against a conventional Fresnel zone plate of the same main focal distance. In our experiment we considered a Fresnel zone plate with 81 zones and the equivalent FraZP constructed by using a triadic Cantor set developed up to stage $S=4$ [i.e., doubling the number of zones of the FraZP in Fig. 1(d)]. The diffractive lenses were printed and then photographically reduced onto 35 mm slides, resulting in a radius $a=2.52$ mm and focal distance $f_{ZP}(\lambda_o)=124$ mm for the design wavelength $\lambda_o=633$ nm. In the experimental setup, a conventional object–lens–image-plane arrangement, the test object was a slide with a set of binary letters. A polychromatic light source (fiber optic illuminator, with a 150 W EKE 3220 K halogen lamp) was employed. The images were obtained directly onto the CMOS detector of a Cannon EOS 350D digital camera with 6.4 μm square pixel size. The distance L between the object and the image plane was fixed to 575 mm, and, to obtain the out of focus images, the distance d from the object plane to the zone plates was varied.

The results are summarized in Fig. 3. Because of the different transmittances of both kinds of lens, the range of intensities of the photographs in this figure were normalized to the peak intensity, but no additional postprocessing was performed. Defocused images obtained with the FraZP show clear improvements when compared with those obtained with the Fresnel zone plate. The improvement is particularly noticeable in terms of the chromatic aberration, even at the focal plane (however, at this plane FraZP pro-

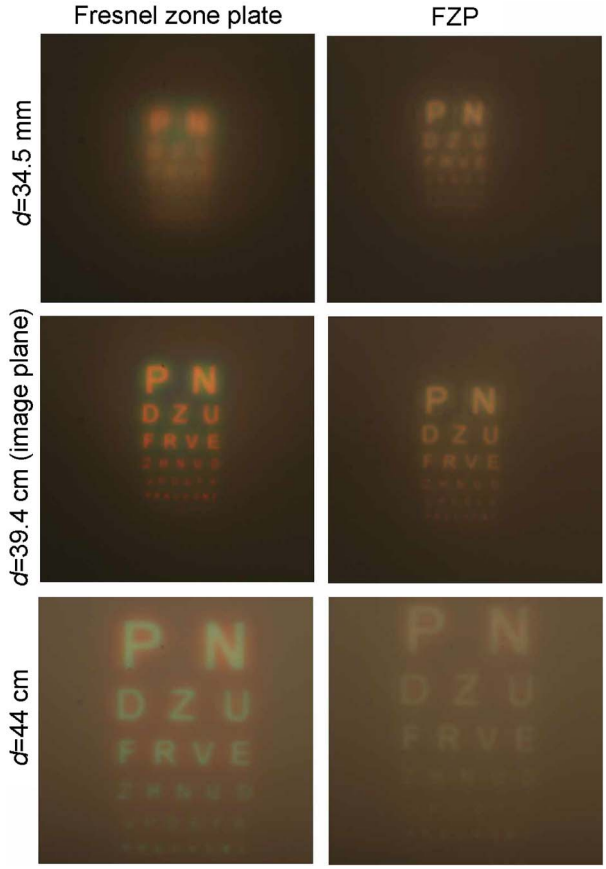

Fig. 3. (Color online) Images obtained with a FraZP and with a Fresnel zone plate. Three different locations for the image plane were considered: in front of the paraxial image plane ($d=44.0$ cm), at the paraxial image plane ($d=39.4$ cm), and behind the paraxial image plane ($d=34.5$ cm).

vides a slightly poor resolution). It can be seen that the depth of field achieved with this plate is larger than the one obtained with Fresnel zone plate. To confirm the result of a subjective comparison, we compute the modulation transfer function (MTF) values for the two lenses under the three experimental conditions. This computational modeling, shown in Fig. 4, accounts for the wideband illumination (wavelengths between 488 and 647 nm) employed in the experiment. The polychromatic MTFs were obtained as the superposition of three monochromatic MTFs (using the same wavelengths as in Fig. 2) weighted by the spectral content of the illumination source and the spectral response of the detector. The results are plotted in Fig. 4. As shown, the MTFs for the defocused planes are about 2 times better for FraZP. Concretely, for the range of frequencies represented in Fig. 4 the ratio between the FraZP and Fresnel zone plate MTFs has the following mean values: 2.41 for $d=345$ mm (defocused plane away from the lens), 0.46 at the focal plane, and 1.73 for $d=440$ mm (defocused plane toward the lens). The improved performance of FraZPs for defocused planes is particularly evident at medium–high frequencies.

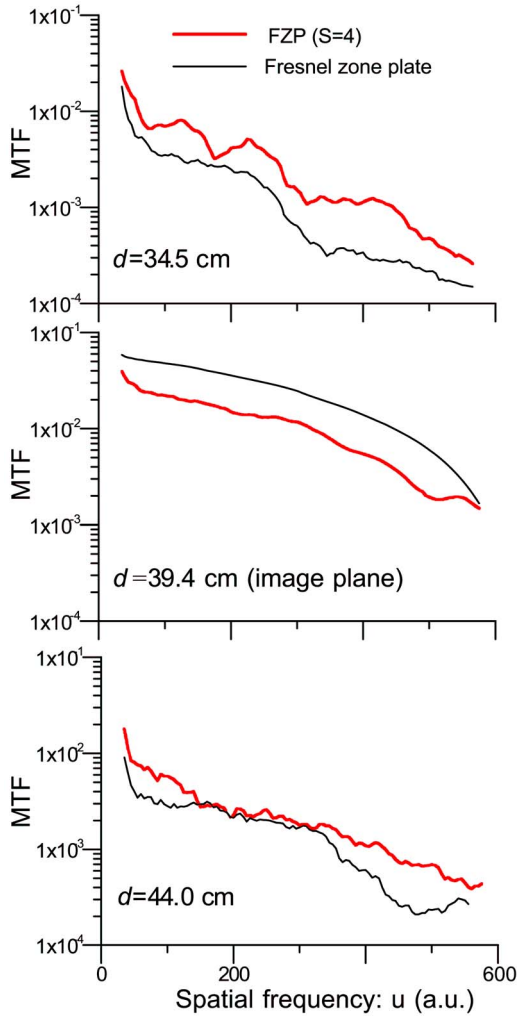

Fig. 4. (Color online) Modulation transfer functions for defocused planes. The MTFs correspond to the three locations of the image planes in Fig. 3.

We believe that the improved imaging capabilities (i.e., an increase in the depth of field and a reduction in the chromatic aberration), shown in Fig. 3 and supported by Fig. 4, that FraZPs offer in polychromatic imaging could be profitable across a broad range of applications where conventional Fresnel zone plates are currently applied, such as x-ray microscopy (where narrowband sources are hardly available), terahertz imaging and tomography, high-energy astronomy, and ophthalmology. Moreover, because FraZPs can be produced by the same techniques used for making Fresnel zone plates, all the improvements already reported for them, such as increasing the resolution by the overlay nanofabrication technique or by the use of composite zones, are still valid for FraZP fabrication. Interestingly, in FraZP design there is an additional parameter, the lacunarity of the fractal function, that adds versatility to the design process because it can modify the number of foci and their relative amplitudes [9].

This research has been supported by the following grants: (1) DPI 2006-8309, Ministerio de Ciencia y Tecnología. Spain; (2) GV/2007/239, Generalitat Valenciana, Spain; (3) “Programa de Incentivo a la Investigación UPV 2005,” Universidad Politécnica de Valencia, Spain.

References

1. Y. Wang, W. Yun, and C. Jacobsen, Nature **424**, 50 (2003).
2. S. Wang, T. Yuan, E. D. Walsby, R. J. Blaikie, S. M. Durbin, D. R. S. Cumming, J. Xu, and X.-C. Zhang, Opt. Lett. **27**, 1183 (2002).
3. E. Di Fabrizio, F. Romanato, M. Gentili, S. Cabrini, B. Kaulich, J. Susini, and R. Barrett, Nature **401**, 895 (1999).
4. R. A. Hyde, Appl. Opt. **38**, 4198 (1999).
5. G. Saavedra, W. D. Furlan, and J. A. Monsoriu, Opt. Lett. **28**, 971 (2003).
6. J. A. Davis, L. Ramirez, J. A. Martín-Romo, T. Alieva, and M. L. Calvo, Opt. Lett. **29**, 1321 (2004).
7. S. H. Tao, X.-C. Yuan, J. Lin, and R. E. Burge, Appl. Phys. Lett. **89**, 31105 (2006).
8. J. A. Monsoriu, W. D. Furlan, P. Andrés, and J. Lancis, Opt. Express **14**, 9077 (2006).
9. J. A. Monsoriu, G. Saavedra, and W. D. Furlan, Opt. Express **12**, 4227 (2004).